Electronic Supplementary Material (ESI) for Physical Chemistry Chemical Physics.

Supporting Information

Effects of Oxygen Vacancy on the Photoexcited Carrier Lifetime in Rutile TiO_2

Lili Zhang[1,2], Weibin Chu[1,3], Qijing Zheng[1*], and Jin Zhao[1,4*]

[1] ICQD/Hefei National Laboratory for Physical Sciences at Microscale, CAS Key Laboratory of Strongly-Coupled Quantum Matter Physics, and Department of Physics, University of Science and Technology of China, Hefei, Anhui 230026, China

[2] Key Laboratory of Material Physics, Ministry of Education, School of Physics and Microelectronics, Zhengzhou University, Zhengzhou 450001, China

[3] Departments of Chemistry, and Physics and Astronomy, University of Southern California, Los Angeles, CA 90089, United States

[4] Synergetic Innovation Center of Quantum Information & Quantum Physics, University of Science and Technology of China, Hefei, Anhui 230026, China

Email: zqj@ustc.edu.cn, zhaojin@ustc.edu.cn

1. Methodology

The ab initio NAMD simulations are carried out using Hefei-NAMD code [1, 2] which augments the Vienna ab initio simulation package (VASP) with the NAMD capabilities within the time-domain density functional theory (TDDFT) similar to Reference [3, 4]. The time-dependent Kohn-Sham (TDKS) orbitals $\psi_e(r,t)$ are expanded in the basis of instantaneous adiabatic Kohn-Sham orbitals $\phi_j(r,R(t))$, which are obtained by solving time-independent Kohn-Sham equation at configuration **R**(t)

$$\psi_e(r,t) = \sum_j c_j(t)\phi_j(r,R(t)) \tag{1}$$

by inserting equation (1) into TDKS equation,[5] a set of differential equations for the coefficients is produced:

$$i\hbar\frac{\partial}{\partial t}c_j(t) = \sum_k c_k(t)\left[\varepsilon_k\delta_{jk} - i\hbar d_{jk}(t)\right] \tag{2}$$

The square modulus of the coefficients $|c_j(t)|^2$ can be explained as the population of the corresponding Kohn-Sham orbitals. Here, ε_k is the energy of the adiabatic Kohn-Sham state and d_{jk} is the NACs between Kohn-Sham states j and k. The NAC can be written as:

$$d_{jk} = \left\langle \phi_j \left| \frac{\partial}{\partial t} \right| \phi_k \right\rangle = \sum_I \frac{\left\langle \phi_j \left| \nabla_{R_I} H \right| \phi_k \right\rangle}{\varepsilon_k - \varepsilon_j} \cdot \dot{R}_I \tag{3}$$

where H is the Kohn-Sham Hamiltonian, ϕ_j,ϕ_k, ε_j, ε_k are the wave functions and eigenvalues for electronic states j and k, and $\dot{R}_I$ is velocity of the nuclei. Thus, the NACs mainly depend on the energy difference term $\varepsilon_k - \varepsilon_j$, the electron-phonon (e-p) coupling term $\left\langle \phi_j \left| \nabla_{R_I} H \right| \phi_k \right\rangle$ and the nuclear velocity term $\dot{R}_I$.

The NACs are calculated in a finite difference method.[6, 7] With the coefficients $c_j(t)$ and the NACs, hopping probabilities between the adiabatic Kohn-Sham states according to Tully's fewest-switches algorithm can be obtained as[8]:

$$P_{j\to k}(t,\Delta t) = \frac{2R\left[c_j^* c_k d_{jk}\right]\Delta t}{c_j^* c_j} \tag{4}$$

Further, the probabilities are multiplied by a Boltzmann factor within the CPA.[3] Besides FSSH, the

decoherence-induced surface hopping was also implemented in Hefei-NAMD.[9]

The decoherence rate is related to the phonon-induced pure-dephasing rate, which can be computed using the optical response theory.[10] In the second-order cumulant approximation, one obtains the unnormalized autocorrelation function (ACF):

$$C(t) = \langle \Delta E(t) \Delta E(0) \rangle$$

where $\Delta E(t) = E(t) - \langle E \rangle$ is the fluctuation of energy gap between two states forming a coherent superposition from its average value. Then, the pure-dephasing function is calculated using as:

$$D(t) = exp\left[-\frac{1}{\hbar^2} \int_0^t dt' \int_0^{t'} dt'' C(t') \right]$$

Generally, *D(t)* decays rapidly, if the initial value of C(t) is large and if C(t) itself also decays rapidly.[11]

2. Test of the supercell size

To check the finite size effects on the oxygen vacancy (O_V) in rutile TiO_2, we calculated the DOS of a 3×3×4 supercell including 216 atoms using DFT+U (U = 4.5 eV for Ti's *3d* orbital) and analyzed the charge distribution of the two excess electrons introduced by the O_V as shown in Figure S1, as compared with those of the 2×2×3 supercell which includes 72 atoms. We can see that the peak positions and charge distribution of defect states using these two supercells are very similar, therefore, we propose that the 2×2×3 supercell is sufficient for the simulation.

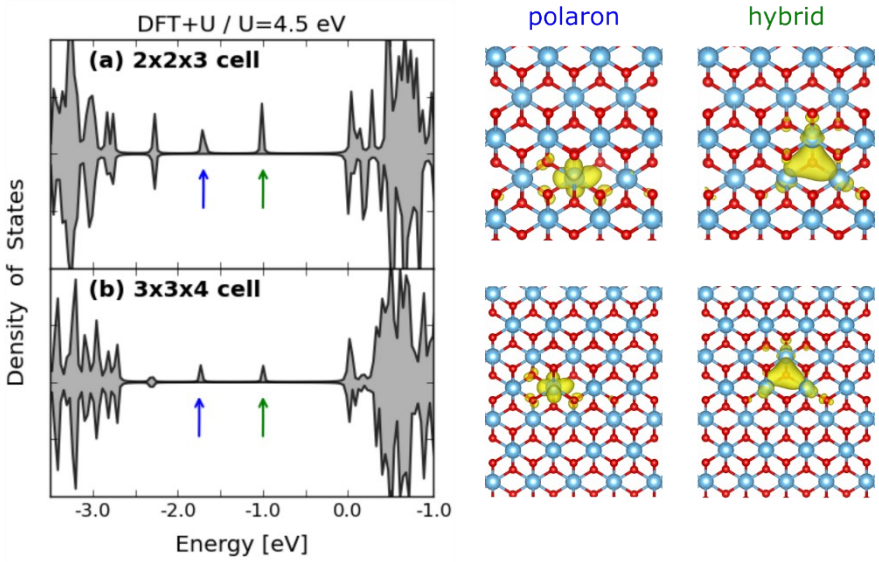

Figure S1. DOS and charge distribution of the two gap states for rutile TiO_2 with O_V in the (a) 2×2×3 and (b) 3×3×4 supercells based on DFT+U calculations (U = 4.5 eV for Ti's *3d* orbital). The isosurface

value is set to 0.004 e/bohr^3.

3. **Test of the U value**

DFT has the well-known self-interaction error and cannot predict the correct band gap of TiO_2. The self-interaction error results in excessive electron delocalization, and therefore, pure DFT functionals cannot achieve the localized polaron state.[12-15] Hybrid functionals or DFT+U can to be used to simulate the small polaron in rutile TiO_2. Calculations with hybrid functionals are very time consuming for periodic systems. Therefore, we use the DFT+U method in our simulation. To check the U value dependence, we calculate using the 2×2×3 supercell for different U values. As shown in Figure S2, we can see that the defect states become deeper in the gap with the increase of the U value. However, the charge distributions of the defect states do not change much. When U value is above 5.5 eV, the defect state peak position become unreasonable. To get a better localization effect of the gap states, therefore, U = 4.5 eV is chosen in our simulation, in accordance with the previous studies.[13, 16]

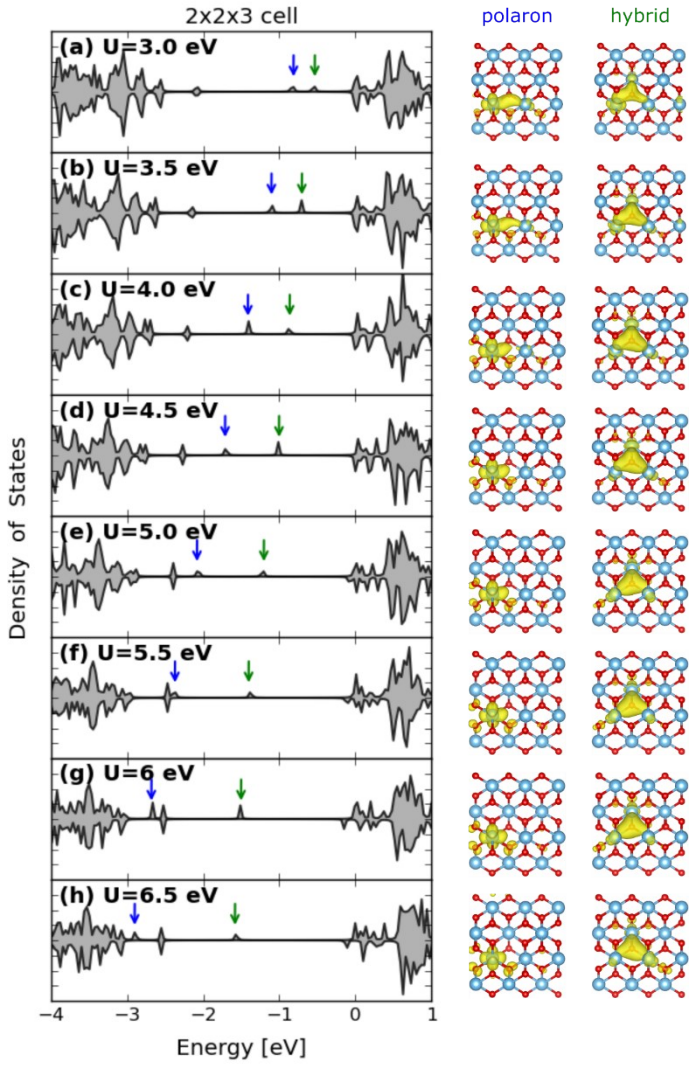

Figure S2. DOS (left) and charge distribution (right) of the two gap states (indicated by blue and green arrows) in rutile TiO_2 with the 2×2×3 supercell obtained using DFT+U with (a) U = 3.0 eV, (b) U = 3.5 eV, (c) U = 4.0 eV, (d) U = 4.5 eV, (e) U = 5 eV, (f) U = 5.5 eV, (g) U = 6 eV and (h) U = 6.5 eV. The isosurface value is set to 0.004 e/bohr^3.

We also compared the DOS and charge density distribution using DFT+U (U=4.5 eV) and HSE06 which is assumed as more accurate calculation method. As shown in Figure S3, the defect states induced by Ov stay in the middle of band gap, although accurate site position is a little different. And the charge density distribution are qualitatively same with one localized state and one hybrid state. However, for MD simulation, hybrid functional method like HSE06 is too cost for nearly 10 ps trajectory. Based on the above statement, we finally choose DFT+U for our calculation.

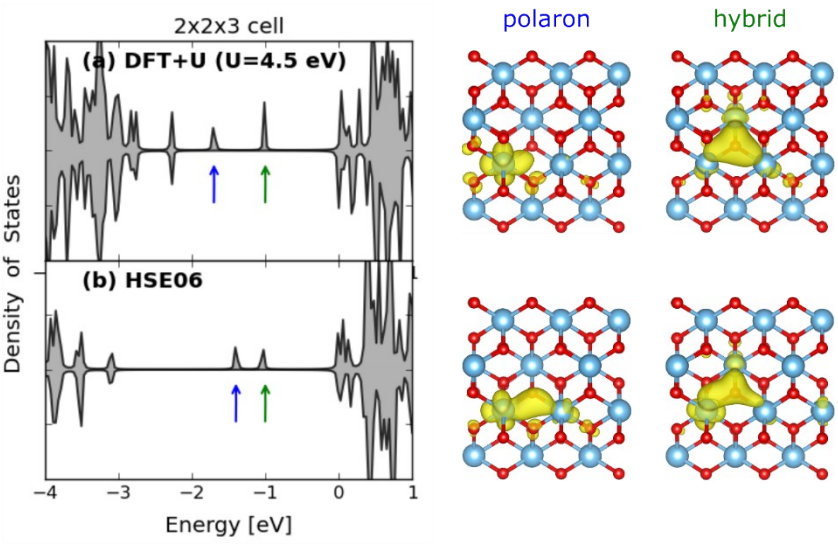

Figure S3. DOS and charge distribution of the two gap states for rutile TiO_2 with 2×2×3 cell including one O_V using (a) DFT+U (U=4.5 eV) and (b) HSE06 methods. The isosurface value is set to 0.004 e/bohr^3.

4. Excess electron induced small polaron

It is known that excess electron can also introduce small polaron in rutile TiO_2. In Figure S4a the DOS of the excess electron induced polaron is shown. It can be seen that a polaron state at -1.2 eV below the CBM is formed. It exhibits a localized distribution on one single Ti atom (labeled as Ti_{15}) as shown in Figure S4b. Table S1 presents the six Ti-O bond lengths around Ti_{xx} with and without polaron formation. It can be seen that the small polaron formation elongates the Ti-O bond length by around 0.1 Å.

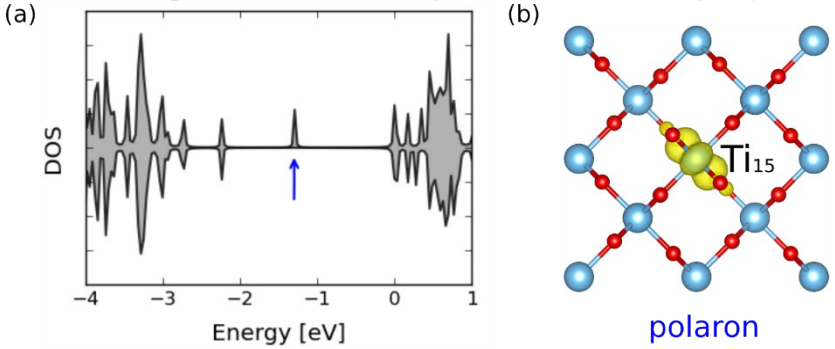

Figure S4. (a) DOS of TiO_2 with one more electron; (b) charge density distribution of polaron state induced by the one extra electron.

The dynamics of excess electron induced polaron is shown in Figure S5. At 100-300 K, the small polaron is mostly localized on Ti_{15}. When the temperature increases to 700 K, the polaron starts to hop

among different Ti atoms. The dynamical behavior is similar with photoexcitation induced small polaron. [17]

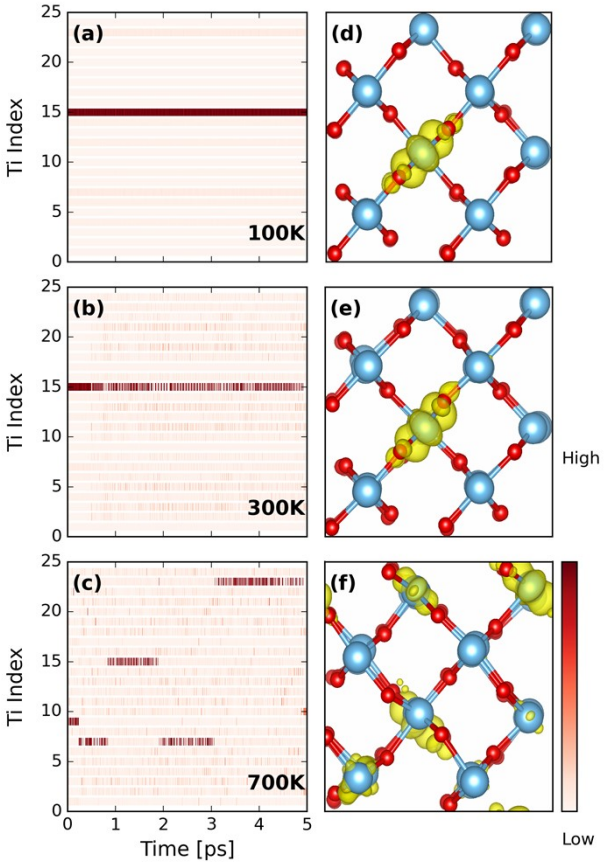

Figure S5. Dynamics of the polaron state at 100, 300 and 700 K. The time dependent charge density localization for the polaron state are shown in (a-c). The corresponding averaged charge distribution are shown in (d-f).

6. State-to-state transition rate and coupled kinetics equations

The inverse of state-to-state relaxation time obtained from fitting the population decays using P(t)=*exp*(-t/τ), as shown in Table S1 below, gives the state-to-state transition rates $k_{state\text{-}to\text{-}state}$. Having established the transition rates between all pairs of states for the pristine TiO_2 and with Ov defect at 100K, 300K, and 700K, we construct a kinetic model to describe the coupled carrier dynamics processes.

(1) The coupled kinetics equations in pristine TiO_2 are:

$$\frac{d[VBM]}{dt} = -k_{(vbm\rightarrow cbm)}[VBM]$$

$$\frac{d[CBM]}{dt} = 1 - [VBM]$$

(2) The coupled kinetics equations in pristine TiO_2 are:

$$\frac{d[VBM]}{dt} = -(k_{(vbm\rightarrow polaron)} + k_{(vbm\rightarrow hybrid)} + k_{(vbm\rightarrow cbm)})[VBM]$$

$$\frac{d[Polaron]}{dt} = k_{(vbm\rightarrow polaron)}[VBM] - k_{(polaron\rightarrow hybrid)}[Polaron] - k_{(polaron\rightarrow cbm)})[Polaron]$$

$$\frac{d[Hybrid]}{dt} = k_{(vbm\rightarrow hybird)}[VBM] + k_{(polaron\rightarrow hybrid)}[Polaron] - k_{(hybrid\rightarrow cbm)})[Hybrid]$$

$$\frac{d[CBM]}{dt} = k_{(vbm\rightarrow cbm)}[VBM] + k_{(polaron\rightarrow cbm)}[Polaron] + k_{(hybrid\rightarrow cbm)})[Hybrid]$$

Table S1 State-to-state transition rate at different temperature.

		Transition Rate $k_{state\text{-}to\text{-}state}$ (ns^{-1})		
		100K	300K	700K
Pristine TiO_2	VBM-CBM	0.26	0.32	1.53
Ov	VBM-Polaron	1.47	9.46	145.90
	VBM-Hybrid	0.24	0.79	5.94
	VBM-CBM	0.22	0.58	1.94
	Polaron-Hybrid	19.46	106.16	2702.70
	Polaron-CBM	1.78	2.93	55.28
	Hybird-CBM	16.46	26.92	335.57

References

1. Zheng, Q.; Zhao, J. Hefei-NAMD. http://staff.ustc.edu.cn/~zhaojin/code.html.

2. Zheng, Q.; Chu, W.; Zhao, C.; Zhang, L.; Guo, H.; Wang, Y.; Jiang, X.; Zhao, J., Ab initio nonadiabatic molecular dynamics investigations on the excited carriers in condensed matter systems. *Wiley Interdiscip. Rev. Comput. Mol. Sci.* **2019,** *0* (0), e1411.

3. Akimov, A. V.; Prezhdo, O. V., The PYXAID Program for Non-Adiabatic Molecular Dynamics in Condensed Matter Systems. *J. Chem. Theo. Comput.* **2013,** *9* (11), 4959-4972.

4. Akimov, A. V.; Prezhdo, O. V., Advanced Capabilities of the PYXAID Program: Integration Schemes, Decoherence Effects, Multiexcitonic States, and Field-Matter Interaction. *J. Chem. Theo. Comput.* **2014,** *10* (2), 789-804.

5. Runge, E.; Gross, E. K. U., Density-Functional Theory for Time-Dependent Systems. *Phys. Rev. Lett.* **1984,** *52* (12), 997-1000.

6. Billeter, S. R.; Curioni, A., Calculation of nonadiabatic couplings in density-functional theory. *J. Chem. Phys.* **2004,** *122* (3), 034105.

7. Hammes-Schiffer, S.; Tully, J. C., Proton transfer in solution: Molecular dynamics with quantum transitions. *J.*

Chem. Phys. **1994,** *101* (6), 4657-4667.

8. Tully, J. C., Molecular-Dynamics with Electronic-Transitions. *J. Chem. Phys.* **1990,** *93* (2), 1061-1071.

9. Jaeger, H. M.; Fischer, S.; Prezhdo, O. V., Decoherence-induced surface hopping. *J. Chem. Phys.* **2012,** *137* (22), 22A545.

10. Mukamel, S. S., *Principles of nonlinear optical spectroscopy*. Oxford University Press: 1995.

11. Akimov, A. V.; Prezhdo, O. V., Persistent Electronic Coherence Despite Rapid Loss of Electron–Nuclear Correlation. *J. Phys. Chem. Lett.* **2013,** *4* (22), 3857-3864.

12. Di Valentin, C.; Pacchioni, G.; Selloni, A., Electronic Structure of Defect States in Hydroxylated and Reduced Rutile TiO_2(110) Surfaces. *Phys. Rev. Lett.* **2006,** *97* (16), 166803.

13. Morgan, B. J.; Watson, G. W., A DFT+U description of oxygen vacancies at the TiO_2 rutile (110) surface. *Surf. Sci.* **2007,** *601* (21), 5034-5041.

14. Stausholm-Moller, J.; Kristoffersen, H. H.; Hinnemann, B.; Madsen, G. K.; Hammer, B., DFT+U study of defects in bulk rutile TiO_2. *J. Chem. Phys.* **2010,** *133* (14), 144708.

15. Park, S.-G.; Magyari-Köpe, B.; Nishi, Y., Electronic correlation effects in reduced rutile TiO_2 within the LDA+U method. *Phys. Rev. B* **2010,** *82* (11), 115109.

16. Calzado, C. J.; Hernández, N. C.; Sanz, J. F., Effect of on-site Coulomb repulsion term *U* on the band-gap states of the reduced rutile (110) TiO_2 surface. *Phys. Rev. B* **2008,** *77* (4), 045118.

17. Zhang, L.; Chu, W.; Zhao, C.; Zheng, Q.; Prezhdo, O. V.; Zhao, J., Dynamics of Photoexcited Small Polarons in Transition-Metal Oxides. *J. Phys. Chem. Lett.* **2021**, 2191-2198.